Available online at www.sciencedirect.com
ScienceDirect
Journal of Nuclear Materials 359 (2006) 162–173
journal of nuclear materials
www.elsevier.com/locate/jnucmat

Cementation of ILW ion exchange resins: Impact of sulfate ions released by radiolysis on hydrated matrix

F. Frizon *, C. Cau-dit-Coumes

CEA Valrhô, DEN/VRH/DTCD/SPDE/L2ED, Bât 37, B.P. 17171, 30207 Bagnols-sur-Cèze cedex, France

Received 9 February 2006; accepted 16 August 2006

Abstract

Some of the ion exchange resins used during treatment of spent nuclear fuels are intermediate level radioactive wastes which may be damaged by radiolysis process, releasing sulfate ions directly into the cement-based encapsulating material. This work consists in an experimental study of the resulting sulfate attack on the properties of the hydrated matrix: dimensional stability, mineralogy and microstructure of the samples, as well as variations in the chemical composition of the curing solution, were studied during six months. Three sites of delayed ettringite formation were detected: into the cement matrix near the surface exposed to solution, localized in the interfacial transition zone between cement matrix and resins, or progressively replacing the portlandite that initially fulfilled the cracks of anionic resins. During the experiment period, the ettringite precipitation and the expansion detected were moderate, and did not lead to cracking. The material involved was considered as having a good resistance to sulfate attack.

PACS: 81.90.+c

1. Introduction

Ion exchange resins, noted here IER, are commonly used during industrial treatment of liquid wastes generated by reprocessing of spent nuclear fuel. These resins are low level or intermediate level radioactive wastes and have to be embedded before being stored. Different encapsulation materials are used such as organic resins (epoxy), or cement based materials. Among the IER conditioning processes, cementation presents the lowest cost, but is confronted with one difficulty: the potential reactivity of encapsulated resins with the cement itself, difficulty that can be solved by a well chosen pretreatment of the IER.

In the case of IER which are intermediate level radioactive wastes, one difficulty is added: due to their organic nature, these resins may be damaged by radiolysis, leading to the degradation of the structure and release of deleterious chemical species in the system. These degradations depend on the integrated dose. Two limit cases may be considered. In the first case, corresponding to a high integrated

* Corresponding author. Tel.: +33 4 66 79 18 83; fax: +33 4 66 39 78 71.
E-mail address: fabien.frizon@cea.fr (F. Frizon).

0022-3115/$ - see front matter © 2006 Elsevier B.V. All rights reserved.
doi:10.1016/j.jnucmat.2006.08.024

dose, the IER have been strongly damaged during storage. Therefore water in contact contains soluble degradation products, which can perturb hydration of cement during the encapsulating process. In the second case, corresponding to a less elevated integrated dose, the IER have been weakly damaged during storage, but degradation may occur in the embedding matrix. The radiolysis products may be released and concentrated into the cement pore solution, leading to a potential perturbation of chemical equilibrium into the material. This may be followed by dissolution of hydrated phases, precipitation of secondary phases and degradation of the matrix at a macroscopic scale.

The IER considered in this paper are constituted by a polystyrenic backbone reticulated with divinylbenzene, which is one of the most common types of resins. This basic structure is functionalized with the addition of sulfonic groups, for cationic resins, or quaternary ammonium groups, for anionic ones. Under radiolysis process, anionic IER release soluble amino-compounds: trimethylamine mainly, but also dimethylamine, monomethylamine or ammonia [1–3], whereas soluble degradation products of cationic ones consist mainly in sulfate ions [2,3]. None of the amino-compounds released is known to have strong interaction with cement-based material, unlike sulfate ions which may strongly interact with cement [4–7]. On the basis of these facts, the present work is focused on the degradation of cationic IER and the interaction of sulfates released on the properties of the cement-based encapsulating matrix. γ-radiolysis of IER and the sulfate attack of cementitious materials are briefly reviewed, before presenting the experimental investigation carried out.

1.1. Degradation of cationic IER under external γ-ray source

Ageing of IER under γ-radiation has been the subject of many studies. Some points are highlighted in the general reviews made by Gangwer et al. [8] and Marsh and Pilay [9].

- Cationic IER resist relatively well to a γ-ray exposition up to a total dose of 1–10 MGy. On the contrary, anionic IER are strongly degraded when the total dose exceeds 0.1–1 MGy.
- IER irradiation causes the break of functional groups and the reticulation and/or degradation of the macromolecular backbone depending on the integrated dose, and in some cases on the dose rate. These degradations affect the exchange capacity and selectivity of IER.
- IER radiolytic degradations increase when the reticulation degree decreases and when water and oxygen are present.

The γ irradiation of cationic resins in presence of water leads to a degradation of the sulphonic functional groups and a release of sulfate ions in solution, those independently of the dose rate. The free sulfate ions concentration varies linearly with the integrated dose up to 5 MGy, then bends slowly and seems to reach a plateau for the very high doses [10]. The maximum sulfate concentration is reached for a degradation of about 33% of the functional groups. This sulfate release corresponds also to a decrease in solution pH and IER exchange capacity.

The resins that are stored in nuclear facilities are of various types and present different integrated doses. In this work, we have chosen to investigate two widely used resins: cationic Amberlite IRN77 and anionic Amberlite IRN78. Their physical and chemical properties are presented in Table 1. Furthermore, the total dose received by IER stored in some French nuclear facilities has been estimated by the year 2010 (Table 2), it would range from 0.06 to 37 MGy, depending on the age and use of IER.

By considering the degradation described in the bibliography [8–10], it was concluded that:

- Major degradations would be expected for group 1 resins. The anionic resins and the older cationic resins (1978 and 1988) would present a high

Table 1
Physical and chemical properties of fresh IER

Name	Amberlite IRN77	Amberlite IRN78
Classification	Cationic strong acid	Anionic base
Functional group	Sulfonic	Quaternary ammonium
Backbone	Polystyrenic gel	Polystyrenic gel
Granule size (mm)	0.3–1.2	0.4–1.2
Density	0.80	0.69
Exchange capacity (eq/kg dry resins)	4.5	3.7
Reticulation degree (%DVB)	8	8

Table 2
Estimation of total dose integrated by two groups of resins by the year 2010

	Sub-group	Storage date	Maximal integrated dose (MGy)
Group 1 Resins	1	1978	37
	2	1988	22
	3	1998	4.2
Group 2 Resins	1	–	0.06
	2	–	0.15
	3	–	0.22

defunctionization rate, and macromolecular backbone scission would be expected for the older resins of both types.
- Minor degradations (partial break of functional groups) would be expected for group 2 resins. Therefore, the degradation may continue after encapsulation, releasing sulfate ions directly into the hydrated cement paste.

1.2. Sulfate attack of hydrated cement based materials

The sulfate attack is a chemical phenomenon leading to degradation of cement-based materials [4] due to expansion, weakening of mechanical resistance [11] and/or breaking up [12] related with crystallization of gypsum and secondary ettringite.

In the case of sulfate attack, ettringite precipitates from calcium and sulfate ions, water molecules and aluminates sources being provided by cement phases, like hydrated calcium monosulfoaluminate, for example (Eq. (1))

$$Ca_4Al_2(OH)_{12}SO_4 \cdot 6H_2O + 2Ca^{2+} + 2SO_4^{2-} + 20H_2O \rightarrow Ca_6Al_2(OH)_{12}(SO_4)_3 \cdot 26H_2O \quad (1)$$

In the previous reaction, aluminates may also be provided by other cement phases, such as anhydrous tricalcium aluminate or hydrated tetracalcium aluminate. Calcium is initially supplied by dissolution of portlandite ($Ca(OH)_2$) up to exhaustion, then by decalcification of calcium silicate hydrate ($(CaO)_X(SiO_2)_Y(H_2O)_Z$ usually noted C–S–H), these two minerals being major components of Ordinary Portland Cement (OPC)-based materials. The sulfate ions may be provided by an external (environmental) source, an internal source (for example sulfate provided by dissolution of primary ettringite due to thermal decomposition of this mineral [13]) or, in the particular case of this study, by radiolysis of cationic IER. External sulfate attack occurs by ingress of reactional front inside the material. Near the surface exposed to the sulfate containing solution, some gypsum may also precipitate.

The swelling due to sulfate attack is a complex phenomenon still poorly understood. Various assumptions, sometime conflicting one with another, have been proposed to explain the link between ettringite precipitation and expansion of the cement-based material.

- Expansive potential of ettringite depends on formation conditions. Many studies show that ettringite is expansive if the pore solution from which it is precipitating is saturated with respect to portlandite [14,15]. These results could be linked to the variation of ettringite solubility as a function of the lime content in solution [16].
- Expansion comes from crystallization pressure. Cracks fulfilled with ettringite in needle form are detected in the case of materials that have been submitted to strong sulfate attack. According to Diamond [5], the growth of these ettringite crystals is responsible for the cracks. According to other authors [17,18] ettringite precipitates initially into microcrystals, causing swelling and cracking of the material. Afterwards, ettringite reprecipitates in needle form in the previously created cracks.
- Expansion results from a modification of C–S–H gel properties. According to Thorvaldson [19], sulfate attack of cement based material is followed by a modification of the chemical environment of C–S–H gel, generating an osmotic pressure leading to a swelling of this gel, and therefore of the whole material.
- Expansion results of water adsorption on colloidal ettringite particle. According to Mehta and co-workers [20–22], this adsorption of water is followed by an increase in the distance between ettringite particles, leading to a swelling of the material.
- Expansion results from water adsorption due to a local dessication of the material. Precipitation of ettringite requires a considerable amount of water. If this amount is not sufficient in the material, the precipitated ettringite could be either partially dehydrated, or totally hydrated by incorporation of water molecules provided by the C–S–H [6]. Swelling is then linked with

water adsorption on ettringite or on C–S–H. However, this fails explaining swelling exhibited by saturated materials.

The relationship between sulfate attack and material expansion is complex, and some of the assumed processes may occur simultaneously depending on the experimental conditions. Independently of the mechanism, swelling seems to be related more to the conditions of ettringite crystallization than to the amount of ettringite precipitated. This formation depends on the composition of anhydrous cement, particularly on its aluminate phases content, and on the presence of addition (blast furnace slag or silica fume for example). A sulfate resistant cement-based material was used to encapsulate IER to ensure a good behaviour under sulfate attack resulting from the radiolytic degradation of cationic resins in the hydrated matrix.

2. Experimental

2.1. Materials involved

The tests were conducted on the one hand on cement coated cationic resins, alone or mixed with anionic resins, and on the other hand on a simplified system consisting in pure hydrated cement. The cement used in this study was a CEM III/C 32.5 PM ES. According to European standards EN 197:1, this cement corresponds to a Blast Furnace Cement consisting of 5–19% Portland Cement Clinker and 81–95% blast furnace slag. The composition is given in Table 3. The use of CEM III/C cement was preferred to CEM I (Ordinary Portland Cement consisting of more than 95% Portland Cement Clinker) because of its better resistance to sulfate attack [23].

The mix of cement and resins is prepared with fresh IER (cf. Table 1) according to the formula summarized in Table 4. The incorporated resins are pure Amberlite IRN77 (cationic resins) and a mix of Amberlite IRN77 and IRN78 with an exchange capacity ratio corresponding to 1/1.

The mix was performed in two steps. The first step consisted in a pre-treatment: resins, calcium nitrate and lime were mixed during 30 min at low speed in a standardized laboratory mixer (European Standard EN 196-1). The second one was the encapsulation operation itself: cement was introduced in the mixer, mixed at low speed for 30 s and at high speed for 3 min.

Table 3
Chemical analyses of the cement used in this study (wt%)

Constituent	Weight%
SiO_2	31.18
Al_2O_3	9.30
Fe_2O_3	1.04
TiO_2	0.45
MnO	0.29
CaO	45.13
MgO	6.52
SO_3	2.95
K_2O	0.50
Na_2O	0.33
P_2O_5	0.06
S^{2-}	0.68
Cl^-	0.02
Loss on ignition	1.54

Table 4
Encapsulation formula used in this study (wt%)

Component	Percent by weight
Dry resins	9.5%
Water	32.5%
$Ca(NO_3)_2$, $4H_2O$	4.2%
$Ca(OH)_2$	2.8%
Cement CEM III/C 32.5 PM ES	51%

The pre-treatment step was designed to achieve three goals:

- to neutralize cationic resins containing H^+, in order to suppress the temperature elevation due to acid–base reaction during hydration of cement,
- to saturate sorption sites of cationic resins with calcium ions. This would limit perturbation during cement hydration, mainly due to a decrease in the calcium concentration in interstitial solution because of its sorption on cationic resins,
- to saturate sorption sites of anionic resins with nitrate ions, in order to avoid the fixation of sulfate ions, which could be released in long-term and promote expansive ettringite formation.

In order to compare the results, some experiments were conducted on pure cement paste, consisting of cement CEM III/C with a water to cement ratio equal to 0.52, which corresponds to the effective w/c ratio of the formulation. The

situation corresponding to a high degradation of the IER was represented by an introduction of sulfate ions directly into the mixing solution at 5.56×10^{-1} mol/L, which corresponds to 2.89×10^{-2} mol for 100 g of cement. This concentration represented the maximum of sulfate that could have been released under γ-radiation with the proposed formula, i.e. a pure cationic IER waste with 33% degradation of functional groups. Table 5 summarizes the nature of the samples used during this study.

Once mixed, samples were cast into cylindrical moulds (9 cm diameter and 12 cm high), and placed into a Langavant semi-adiabatic calorimeter. During the first days and due to the exothermic hydration reactions, they were submitted to a temperature elevation representative of the heating expected in real casting conditions in the containers (Fig. 1). These curves showed two major results. First, with increasing IER volume, i.e. from tests I and II containing no ion exchange resins to test VII embedding Amberlite IRN77 and IRN78, going through test IV, V and VI encapsulating only Amberlite IRN 77, the thermal variation decreased. Second, the cement paste mixed with the sodium sulfate solution (test III) showed the highest and fastest thermal variation, probably due to an acceleration of hydration caused by alkali-activation of blast furnace slag from cement CEM III [24]. As previously highlighted, this thermal historical background is of primary importance in delayed ettringite formation [13,25]. It can be noticed that the temperature rise remained moderate for most samples (below 45 °C), which should limit the thermal decomposition of ettringite followed by delayed recrystallization and potential expansion.

The sample were then placed into airtight bag and stored at 20 °C during 260 days. This maturation period allowed reaching a significant hydration level of blast furnace cement, the hydration kinetics of which is slow. After this period, samples were cut to obtain thin plates (10 * 4 * 0.5 cm). This particular shape was chosen to minimize the time needed for ions to diffuse into the cement-based materials.

2.2. Experimental processes

In the real case of γ-ray degradation of cement coated resins, sulfate ions would be progressively released directly into the hydrated matrix. As progressive releasing of sulfate ions directly into the matrix is very difficult to simulate during laboratory experiments, tests were conducted under the following conditions: thin samples were placed into an aqueous solution containing sulfate ions at a concentration corresponding to the amount that could be released under radiolysis. Table 5 summarizes the tests conducted with these samples. The volume ratio of storing solution on samples was fixed between 1.4 and 1.6; it had to be sufficient to ensure a total immersion of the sample, and to be as low as possible to limit the leaching of the material. The experiments were conducted in airtight cells during 6 month and without solution renewing. The carbonation of the samples was controlled at the end of the experiment.

Tests I and IV were reference experiments. Tests II and III were dedicated respectively to the evaluation of external and internal sulfate attack resistance of the selected cement; in the first case sulfate ions

Table 5
Tests conducted. Materials and solutions involved

Test number	Nature of the samples	Storing solution
I	Cement paste CEM III/C – w/c 0.52	Ultrapure water
II	Cement paste CEM III/C – w/c 0.52	Na_2SO_4 containing solution. The sulfate concentration in solution corresponds to 2.89×10^{-2} mol for 100 g of cement
III	Cement paste CEM III/C – w/c 0.52 Na_2SO_4 in mix water (2.89×10^{-2} mol of SO_4^{2-} for 100 g of cement)	Ultrapure water
IV	Amberlite IRN77 encapsulation material	Ultrapure water
V	Amberlite IRN77 encapsulation material	Na_2SO_4 containing solution. The sulfate concentration in solution corresponds to 2.89×10^{-2} mol for 100 g of cement
VI	Amberlite IRN77 encapsulation material	NaOH containing solution. The sodium concentration in solution corresponds to 5.78×10^{-2} mol for 100 g of cement
VII	Amberlite IRN77 and IRN78 encapsulation material	Na_2SO_4 containing solution. The sulfate concentration in solution corresponds to 1.30×10^{-2} mol for 100 g of cement

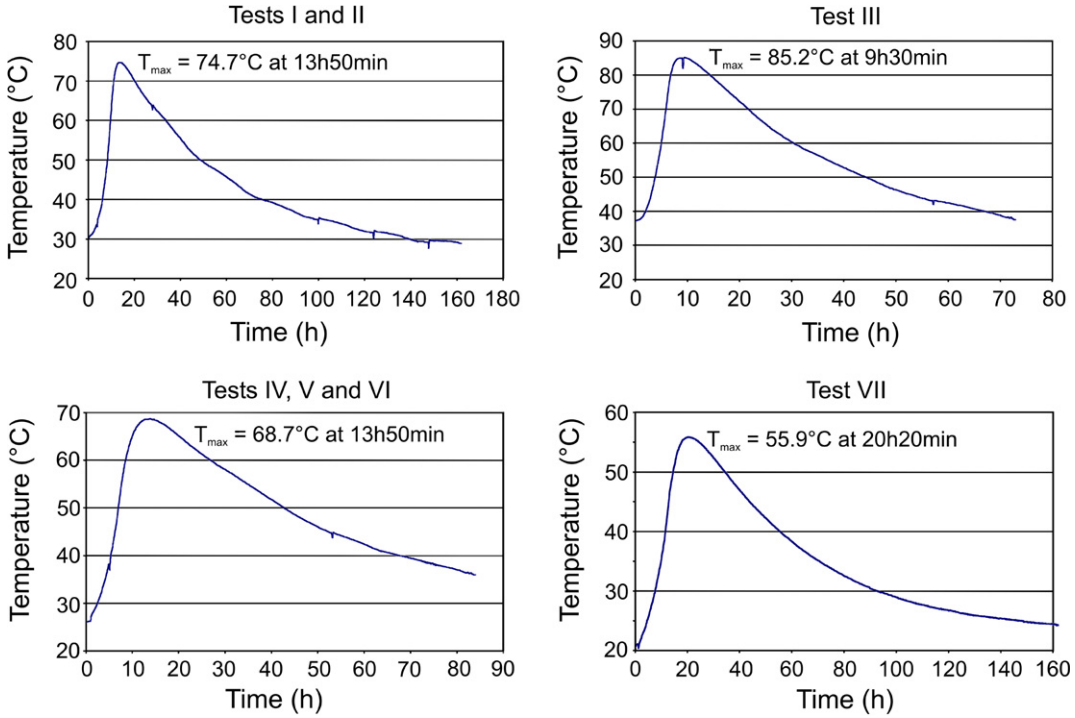

Fig. 1. Thermal variations of the samples due to cement hydration. The curve corresponding to tests I and II is obtained from a pure cement paste with w/c = 0.52. The curve corresponding to test III is obtained from a cement paste (w/c = 0.52) containing Na_2SO_4 in mix water. The curve corresponding to tests IV, V and VI is obtained from an Amberlite IRN 77 encapsulation material. The curve corresponding to test VII is obtained from an Amberlite IRN 77 and IRN 78 encapsulation material. Please refer to Table 5 for more details.

could interact with cement hydrated phases, in the second one sulfate ions were involved in cement hydration. The amount of sulfates corresponded to a waste consisting exclusively of cationic resins presenting a 33% degradation of the functional groups.

Sulfate attack on the cement matrix, designed according to the formula given in Table 4, was investigated with tests IV to VII. Test V corresponded to an encapsulation of pure cationic resins, whereas test VII, corresponding to a mix between anionic and cationic IER, was the most representative experiment of real waste encapsulation. In order to evaluate the possible influence of sodium ions on material stability during test V, an experiment involving sodium ions was also conducted (test VI). The quantity of sodium was equal to that used in test V.

2.3. Analytical methods

Evolution of materials and storing solutions with time was monitored by performing a set of analyses: dimensional stability, mineralogy, microstructure, porosity and portlandite content of the material and composition of storing solution.

Dimensional stability of the samples was measured by swelling sensors interfaced with a computer that was recording one value every 30 min.

Mineralogy of the samples was determined using X-ray diffraction. The powder diffractograms were obtained using a Brücker D8 diffractometer with Cu Kα radiation ($\lambda K\alpha 1 = 1.54056$ Å) generated at 40 mA and 40 kV. Specimens were scanned from 10° to 60° 2θ at 0.02° 2θ steps integrated at the rate of 2 s per step.

Microstructure was investigated using a Jeol JSM 820 scanning electron microscope (SEM) equipped with an energy dispersive analyzer (EDS). These observations were conducted on sample cracks under secondary electrons operating at 15 kV.

Porosity was characterized by mercury intrusion using a Micromeritics Autopore III 9420, pressure varying from 0.8 to 530 000 psia.

The amount of portlandite in the material was determined using differential thermal analyses

TDA/TGA (Setaram SDT 2960) with an investigated range of temperature for 40–800 °C and a slope of 10 °C/min.

The composition of storing solution in term of Na^+, K^+, Ca^{2+}, NO_3^-, SO_4^{2-} was analyzed by ionic chromatography (Dionex DX 500), while pH was measured with a pH meter (Consort C831) equipped with high alkalinity pH sensor (Metrohm Unitrade).

3. Results and discussion

3.1. Cement pastes

Fig. 2 represents the dimensional variations of samples submitted to tests I, II and III. The three curves followed the same trend: during the first week, a quick swelling appeared, corresponding to about a half of the total observed expansion, then during three months, the swelling slowed down and seemed to be stabilized after this period. The first phase is probably associated with diffusion and capillary suction of water into porosity, leading to a relaxation of shrinkage forces due to self-desiccation. Osmotic pressure due to concentration gradients between the pore solution and the curing solution might also be observed especially for test III. The swelling values reached in the plateau were however different from one sample to another. Indeed, the swelling of CEM III paste stored in sodium sulfate solution (about 500 μm/m) presented an expansion comparable with the reference stored in ultrapure water (about 600 μm/m). The paste mixed with sodium sulfate solution presented unlike the others a much higher swelling: about 1400 μm/m. No cracks were however observed after 6 months of storage.

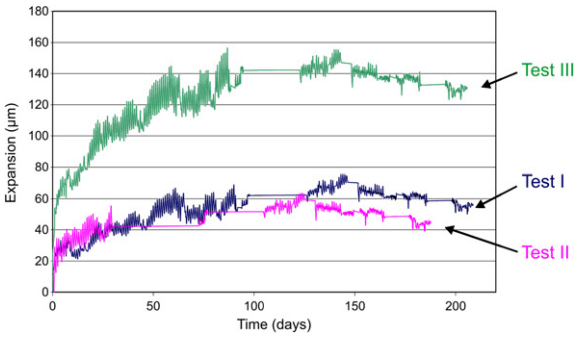

Fig. 2. Influence of sulfate on longitudinal expansion of CEM III/C paste with water to cement ratio equal to 0.52. Tests I and II consist of pure cement paste stored respectively in ultrapure water and Na_2SO_4 containing solution. Test III consists of a cement paste mixed with Na_2SO_4 containing mix water stored in ultrapure water. The flat parts correspond to a break in data acquisition. Please refer to Table 5 for more details.

Monitoring the chemical evolution of the investigated systems provided interesting information. The results obtained on solids at 0 and 6 months by TDA/TGA analyses are summarized in Table 6.

At the immersion time, the CEM III paste mixed with sodium sulfate solution seemed to present a higher degree of hydration than pastes mixed with pure water. There was indeed no signal corresponding to portlandite for test III (portlandite is an hydrate formed in the early stage of hydration of CEM III) and the mass loss due to hydrated phases was more important than that of the reference. This result may be explained by two different ways: on the one hand sodium and sulfate ions are activators of blast furnace hydration, thus promoting high hydration rates [24]; on the other hand, the material contains more ettringite than the reference (ettringite is a water-rich phase containing 32 molecules of water in its structure). These two assumptions are also in agreement with the fact that the finest porosity is observed for the sample coming from test III

Table 6
Thermogravimetric analysis of samples from tests I, II and III at 0 and 6 months

Analysis date	Test I		Test II		Test III	
	0 month	6 months	0 month	6 months	0 month	6 months
Free water <80 °C	1.6	2.3	1.6	2.1	1.6	2.1
Bound water from 80 to 630 °C	16.6	23.7	16.6	22.6	20.3	24.6
coming from portlandite	0.6	0.5	0.6	0.4	–	–
Mass loss from 630 to 1000 °C	0.9	0.7	0.9	0.5	0.7	0.4
coming from CO_2 due to calcite	0.8	0.6	0.8	0.5	–	–
Total loss	19.1	26.7	19.1	25.2	22.6	27.1

The mass losses are indicated in %. The time origin corresponds to the immersion of the samples into curing solution (273 days old cement pastes).

(Table 7). After 6 months of curing, the progress of hydration was noticed for all samples: the portlandite content decreased, while the bound water increased. The lower portlandite content in test II compared with reference test I is probably associated to conversion of portlandite into other calcium containing phases (C–S–H, ettringite,...): no increasing concentration of calcium was indeed detected in the storing solution (Table 8), thus indicating that portlandite had not simply dissolved into water due to leaching.

Concerning storing solutions analyses presented in Table 8, some points may be highlighted. First, considering test II results, a decrease in sulfate and sodium concentrations was observed with increasing time. This reduction may be linked either to consumption due to precipitation of sulfate and/or sodium containing phases or to dilution by interstitial solution of the cement paste. Second, the amount of sulfate released after 6 months in the storing solution during test III corresponded to 16% of the total sulfate concentration initially introduced in mix water, proving that this chemical specie was not fully integrated in the hydrated phases of cement. If we are considering sodium ions, the amount released after 6 months reached 50% of total sodium ions initially introduced. This difference reveals that sodium and sulfates in the curing solution did not simply result from the dissolution of Na_2SO_4.

From a mineralogical point of view, the same crystalline phases were detected in all the tests. X-ray diffraction allowed to identify: amorphous compounds (C–S–H, blast furnace slag), hydrotalcite, ettringite, calcite, and calcium silicates that were still not hydrated. Presence of ettringite was expected even in the reference material: this phase is indeed one of the CEM III hydration products. Portlandite revealed by thermodifferential analyse was not detected by XRD because of its low concentration in the material which was below the XRD detection limit. No mineralogical evolution was subsequently detected.

The microstructural evolution of the materials with time was observed by SEM on sample fractures at different ages. Concerning test I samples, no notable microstructural evolution was observed. All analyses revealed compact C–S–H, some massive portlandite crystals and ettringite in needle form mainly in air bubbles. Moreover, no microstructural

Table 7
Porosity analysis of samples from tests I, II and III at 0, 3 and 4 months

	Analysis date (days)	Total porosity (%)	<15 nm	15–200 nm% of total porosity	>200 nm
Test I	0	41	33	63	4
	90	40	37	62	1
	120	41	42	57	1
Test II	0	40	33	63	4
	90	40	40	58	2
	120	41	41	54	5
Test III	0	34	41	59	0
	90	41	49	49	2
	120	43	56	41	3

Table 8
Chemical composition evolution of the storing solutions used in tests I–III

	Analysis date	pH	Na^+ (mg/L)	K^+ (mg/L)	Ca^{2+} (mg/L)	NO_3^- (mg/L)	SO_4^{2-} (mg/L)
Test I	0 month	–	0	0	0	0	0
	6 months	12.2	245	475	40	0	53
Test II	0 month	–	9800	0	0	0	20448
	6 months	12.5	8086	541	20	0	15251
Test III	0 month	–	0	0	0	0	0
	6 months	12.9	3980	697	23	0	2593

Concentrations values obtained by ionic chromatography and expressed in mg/L ± 10%.

change appeared between the bulk and the surface of the sample exposed to water. The situation was quite different for test II samples: the bulk material morphology was similar to the probe, i.e. dense with C–S–H, portlandite and ettringite in needle form, but near the surface exposed to the sulfate-containing storing solution, some massive ettringite crystals were detected.

The zone containing these crystals seemed to thicken with time and, after six months, finally reached about 100–200 μm. The amount of ettringite in the sample was too low to explain the macroscopic expansion detected, which may still be associated with relaxation of self desiccation constraints as previously discussed. Test III samples followed the same trend as the probe: no microstructural change was observed, neither with time nor depth. In these samples, the matrix was however different and consisted mainly in compact C–S–H and massive ettringite, some crystals in needle form were also found in air bubbles.

3.2. Encapsulating materials

Concerning the encapsulation materials, dimensional variations of samples submitted to tests IV, V, VI and VII are presented in Fig. 3.

These recorded curves are similar to those previously described for pure cement pastes. The samples exhibited a quick swelling during the first weak of immersion which then slowed down and finally

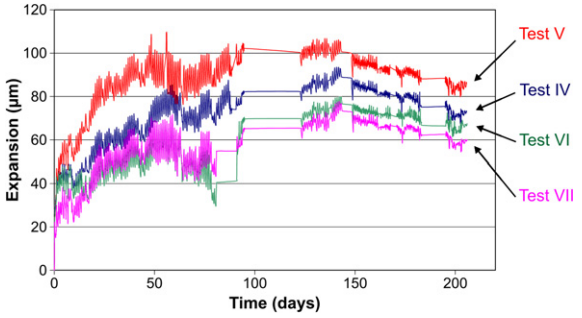

Fig. 3. Influence of sulfate in storing solution on longitudinal expansion of encapsulating materials. Test IV consists of Amberlite IRN77 encapsulation material stored in ultrapure water. Test V consists of Amberlite IRN77 encapsulation material stored in Na_2SO_4 containing solution. Test VI consists of Amberlite IRN77 encapsulation material stored in NaOH containing solution. Test VII consists of Amberlite IRN77 and IRN78 encapsulation material stored in Na_2SO_4 containing solution. The flat parts correspond to a break in data acquisition. Please refer to Table 5 for more details.

reached a plateau after 3 months. Moreover the expansion values reached by the samples were close from each other (about 900 μm/m for test V sample, 800 μm/m for the probe, 700 μm/m and 600 μm/m respectively for test VI and test VII). Furthermore, no cracks were detected after six months of immersion in storing solution. Therefore, the expansion observed is attributed to diffusion and capillary suction of water into porosity, leading to a relaxation of shrinking forces, and to a development of osmotic pressure due to the concentration difference between the pore and the curing solution.

Due to the presence of resins in the materials, TDA and porosity analyses were impossible. However, the storing solutions could be analysed; results obtained at starting time and after six months of immersion are summarized in Table 9.

The storing solution from test IV presented after 6 months a high content of nitrate and calcium resulting from resins pre-treatment. A total release of these ions in the storing solution should have led to much higher concentrations (1160 and 18 760 mg/L respectively in calcium and nitrate), these species must have therefore taken part in cement hydration. Concerning test V solution, the most notable point was the decrease in the sodium and sulfate concentrations after six months of storage. This point may be explained by several hypotheses: a dilution of the storing solution by the encapsulating material pore solution, an incorporation of these ions into the material solid structure or a fixation of sodium on cationic resins. The same explanations may also legitimate the decrease in the hydroxyl and sodium concentrations in test VI storing solutions, but are unable to explain the difference existing between the decreases in sulfate concentration observed in tests VII and V. In that later case, a possibility for sulfate to fix on Amberlite IRN78 anionic resins may also contribute to this concentration reduction.

The XRD diffractogramms obtained on the materials showed no difference whatever the test or the curing time. All encapsulation materials included amorphous compounds (C–S–H, blast furnace), hydrotalcite, tricalcium and dicalcium silicates that were still not hydrated, calcite and ettringite.

The microstructure presented by the cement matrix of samples submitted to tests IV and VI was similar to that of the cement paste investigated in test I, i.e. compact with C–S–H, some massive portlandite crystals and ettringite in needle form in air bubbles. The principal difference was observed

Table 9
Chemical composition evolution of the storing solutions used in tests IV–VII

	Analysis date	pH	Na^+ (mg/L)	K^+ (mg/L)	Ca^{2+} (mg/L)	NO_3^- (mg/L)	SO_4^{2-} (mg/L)
Test IV	0 month	–	0	0	0	0	0
	6 months	11.8	356	568	841	3919	<d.l.
Test V	0 month	–	6900	0	0	0	14400
	6 months	11.9	4424	462	46	8638	3120
Test VI	0 month	13.3	6854	0	0	0	0
	6 months	12.6	3596	375	171	7335	96
Test VII	0 month	–	2880	0	0	0	6010
	6 months	12.4	2050	463	18	4150	407

Concentrations values obtained by ionic chromatography and expressed in mg/L ± 10%.

at the resin–cement interface: the transition zone was of poor cohesion. This particular point is probably linked to the contraction of resins caused by sample desiccation during their preparation for SEM observation. Increasing immersion time in storing solution did not result in any change. On the contrary, test V sample had a time dependant behaviour: as for test II samples, massive ettringite was located in a zone situated near the surface exposed to storing solution. This zone seemed to thicken with time and finally reached 100–200 μm after six months. This ettringite formation may contribute to the decrease in the calcium concentration observed in storing solution analyses (cf. Table 9), but remains too low to induce abnormal macroscopic expansion (Fig. 3).

Behaviour of sample submitted to test VII was different. First of all, anionic resins presented cracks, initially fulfilled with portlandite. The links between portlandite precipitation and cracking of resin may be considered with two hypotheses:

- portlandite precipitates preferentially into pre-existing cracks: functional groups of anionic resins may be saturated with hydroxyl ions; this local over concentration could lead to portlandite precipitation. This point is in agreement with the lower mechanical strength noticed for anionic resins as compared with cationic ones,
- portlandite precipitates preferentially near anionic resins because of a local over concentration in hydroxyl. The crystallization pressure would then lead to cracking of the resins.

However with increasing immersion time, portlandite was progressively replaced by ettringite. Ettringite solubility is indeed low in presence of portlandite [16], which could explain this localized precipitation. Furthermore, some ettringite crystals in needle form were founded on the sample surface exposed to sulfate solution, in addition to the massive ettringite zone already noticed. Nevertheless, the amount of ettringite formed during storage was insufficient to induce abnormal expansion.

4. Conclusion

Cement-based materials are extensively used to encapsulate ion exchange resins used during industrial treatment of spent nuclear fuel. Some of these resins are intermediate level radioactive wastes, which may be damaged by radiolysis process, releasing sulfate ions from the functional groups directly into the cement based encapsulation material. This process being difficult to simulate in a laboratory experiment, conservative trials were carried out by placing thin platelet cement samples into a small volume of solution containing the amounts of sulfate which would be produced by total degradation of the IER. The main achieved results can be summarized as follows.

The attack of a CEM III/C paste (water to cement ratio equal to 0.52) by a sodium sulfate solution (2.89×10^{-2} mol/100 g of cement) leads to secondary ettringite formation near the surface exposed to the storing solution. The thickness of this zone varies between 100 μm and 200 μm after 6 months of experiment. Unlike primary ettringite crystallized in needle form in air bubbles, secondary ettringite precipitated in massive crystals, perfectly mixed with C–S–H. Its formation seemed to start as soon as the experiments began and consumed a part of the portlandite present into hydrated cement. The small amount of precipitated ettringite

was insufficient to lead to macroscopic swelling of the sample: longitudinal expansion of the samples was comparable to that of a reference sample stored under ultrapure water, and could result from:

- for the first weeks, the relaxation of shrinkage constraint associated with self desiccation of the material,
- during experiment duration, the development of osmotic pressure.

Concerning the opposite case where sulfates were added to the mixing water and the paste stored into ultrapure water, three main effects were detected:

- Cement hydration seemed to be accelerated.
- There was more primary ettringite in the hydrated material than in the probe mixed with pure water.
- The pore distribution was finer due to hydration acceleration and/or filling of the voids by primary ettringite precipitation.

During immersion, the material had an expansion as high as that of the reference. However this swelling was not associated with any cracking of the paste.

In conclusion, on the experiment duration, the cement paste presented a good resistance to external and internal sulfate attack.

Sulfate attack of cement pastes encapsulating cationic resins led to the same phenomena as, i.e. precipitation of secondary massive ettringite near the surface exposed to storing solution. The thickness of this zone reached 100–200 μm after six months of experiment. This formation of ettringite was however insufficient to lead to any deleterious swelling of the material. The longitudinal expansion observed after six months was in good agreement with that of the reference stored in ultrapure water.

The more striking modifications were observed on the encapsulation material of a mix of cationic and anionic IER stored in sodium sulfate solution. SEM analyses before immersion revealed that many anionic resins were cracked. These cracks were fulfilled with portlandite. After immersion in sodium sulfate solution, secondary ettringite formation was observed:

- on the surface exposed to storing solution,
- in the material, at the transition zone between resin and cement or in replacement of portlandite in the anionic resins cracks.

This secondary ettringite precipitated in needle form and did not appear to be expansive. The longitudinal expansion reached after six months remained lower than that of the material encapsulating cationic resins and stored in pure water.

As a conclusion, on the experiment duration, the resins encapsulating materials also presented a good resistance to external sulfate attack.

Acknowledgements

The authors gratefully acknowledge AREVA-NC for their financial support to this research.

References

[1] G.R. Hall, M. Streat, J. Chem. Soc. 5 (1963) 5205.
[2] K.J. Swyler, C.J. Dodge, R. Dayal, Irradiation effects on the storage and disposal of radwaste containing organic ion-exchange media, Brookhaven National Laboratory, Report NUREG/CR-3383 DE84 008677, 1983.
[3] L.R. Van Loon, W. Hummel, The radiolytic and chemical degradation of organic ion exchange resins under alkaline conditions: effect on radionuclide speciation, Paul Scherrer Institute, Technical Report 95-08, 1995.
[4] J. Skalny, J. Marchand, I. Adler, Sulfate attack on concrete, London, 2002.
[5] S. Diamond, Cem. Concr. Comp. 18 (3) (1996) 205.
[6] P.E. Brown, H.F.W. Taylor, in: J. Marchand, J.P. Skalny (Eds.), Materials Science of Concrete: Sulfate Attack Mechanisms, The American Ceramic Society, Westerville, OH, 1999, p. 73.
[7] D. Planel, Les Effets Couplés de la Précipitation d'Espèces Secondaires sur le Comportement Mécanique et la Dégradation Chimique des Bétons, PhD thesis, Université de Marne-la-Vallée, France, 2002 (in French).
[8] T.E. Gangwer, M. Goldstein, K.K.S. Pilay, Radiation effects on ion exchange materials, Brookhaven National Laboratory, Report BNL-50781-UC-70, 1977.
[9] S.F. Marsh., K.K.S. Pilay, Effects of ionizing radiation on modern ion exchange materials, Los Alamos National Laboratory, Report LA-12655-MS, 1993.
[10] K.J. Swyler, C.J. Dodge, R. Dayal, Assessment of irradiation in radwaste containing organic ion-exchange media, Brookhaven National Laboratory, Topical Report NUREG/CR-3812, 1984.
[11] P.W. Brown, Cem. Concr. Res. 11 (1981) 719.
[12] P.K. Mehta, in: J. Skalny (Ed.), Material Science of Concrete III, American Ceramic Society, Westerville, OH, 1992, p. 105.
[13] D.W. Hobbs, in: B. Erlon (Ed.), ACI SP-177, Ettringite – The Sometimes Host of Destruction, American Concrete Institute, Farmington Hills, MI, 1999, p. 159.
[14] T. Nakamura, G. Sudoh, S. Akaiwa, in: Proceedings of the 5th International Symposium on the Chemistry of Cement, Tokyo, 1968, p. 351.
[15] D. Min, T. Mingshy, Cem. Concr. Res. 24 (1) (1994) 119.
[16] R. Duval, H. Hornain, in: J. Baron, J.P. Ollivier (Eds.), La Durabilité des Bétons, Presses de l'Ecole Nationales des Ponts et Chaussées, Paris, 1992, p. 351.

[17] B. Erlin, in: L. Jany, A. Nisperos, J. Baykes (Eds.), Proceedings of the 18th International Conference on Cement Microscopy, International Cement Microscopy Association, Duncanville, TX, USA, 1996, p. 380.
[18] V. Johansen, N. Thaulow, J. Skalny, Adv. Cem. Res. 5 (17) (1993) 23.
[19] T. Thorvaldson, in: Proceedings of the 3rd International Symposium on the Chemistry of Cement, Cement and Concrete Association, London, 1954, p. 436.
[20] P.K. Mehta, Cem. Concr. Res. 3 (1973) 1.
[21] P.K. Mehta, F. Hu, J. Am. Ceram. Soc. 61 (1978) 179.
[22] P.K. Mehta, S. Wang, Cem. Concr. Res. 12 (1) (1982) 121.
[23] M. Regourd, H. Hornain, P. Levy, B. Mortureux, in: 7eme Congrès International de la Chimie du Ciment, Paris, 3, 1980, p. 104.
[24] H.F.W. Taylor, Cement Chemistry, 2nd Ed., Thomas Telford, London, 1997.
[25] R. Barbarulo, H. Peycelon, S. Prené, J. Marchand, Cem. Concr. Res. 35 (2005) 125.